Earth and Planetary Science Letters 560 (2021) 116790

Contents lists available at ScienceDirect

Earth and Planetary Science Letters

www.elsevier.com/locate/epsl

How is sea level change encoded in carbonate stratigraphy?

Emily C. Geyman [a,*], Adam C. Maloof [a], Blake Dyer [a,b]

[a] Department of Geosciences, Princeton University, Princeton, NJ, United States of America
[b] Department of Earth and Ocean Sciences, University of Victoria, Victoria, BC, Canada

ARTICLE INFO

Article history:
Received 14 September 2020
Received in revised form 29 December 2020
Accepted 26 January 2021
Available online xxxx
Editor: J.P. Avouac

Keywords:
carbonates
cycles
stratigraphy
sedimentary facies
Bahamas

ABSTRACT

The history of organismal evolution, seawater chemistry, and paleoclimate is recorded in layers of carbonate sedimentary rock. Meter-scale cyclic stacking patterns in these carbonates often are interpreted as representing sea level change. A reliable sedimentary proxy for eustasy would be profoundly useful for reconstructing paleoclimate, since sea level responds to changes in temperature and ice volume. However, the translation from water depth to carbonate layering has proven difficult, with recent surveys of modern shallow water platforms revealing little correlation between carbonate facies (i.e., grain size, sedimentary bed forms, ecology) and water depth. We train a convolutional neural network with satellite imagery and new field observations from a 3,000 km^2 region northwest of Andros Island (Bahamas) to generate a facies map with 5 m resolution. Leveraging a newly-published bathymetry for the same region, we test the hypothesis that one can extract a signal of water depth change, not simply from individual facies, but from sequences of facies *transitions* analogous to vertically stacked carbonate strata. Our Hidden Markov Model (HMM) can distinguish relative sea level fall from random variability with ~90% accuracy. Finally, since shallowing-upward patterns can result from local (autogenic) processes in addition to forced mechanisms such as eustasy, we search for statistical tools to diagnose the presence or absence of *external* forcings on relative sea level. With a new data-driven forward model that simulates how modern facies mosaics evolve to stack strata, we show how different sea level forcings generate characteristic patterns of cycle thicknesses in shallow carbonates, providing a new tool for quantitative reconstruction of ancient sea level conditions from the geologic record.

1. Introduction

Shallow-water carbonates are one of the most abundant archives of Earth history (Peters and Husson, 2017). Carbonates are unique because they encode information about both seawater chemistry—through properties such as mineralogy and isotopic composition—and the physical environment—through the sedimentary *facies*. Facies can include all physical, chemical, and biological observables, but in practice (in the geological record), typically incorporate grain size and composition, sedimentary bedforms, and trace and body fossils.

In ancient shallow carbonates, particular sequences of facies, known as *shallowing-upward parasequences*, commonly are interpreted as representing relative sea level fall, which could reflect eustasy or simply the filling of available accommodation space (Grotzinger, 1986; Goldhammer et al., 1990; Read et al., 1986; Koerschner and Read, 1989; Fischer, 1964; Osleger and Read, 1991). When dozens or hundreds of these meter-scale parasequences are stacked together, a canonical interpretation is that such sequences record periodic oscillations in global sea level. These meter-scale parasequences form the building blocks of stratigraphic interpretation, from making inferences about paleoclimate to tuning sections to astrochronological timescales. However, over the last few decades, several separate lines of evidence have cast doubt on the notion that meter-scale parasequences record eustatic sea level change.

1. **Are facies reliable recorders of water depth?** The first major challenge comes from observations of modern carbonate environments. Surveys from the Bahamas (Harris et al., 2015), Florida (Rankey, 2004), and the Red Sea (Purkis et al., 2014, 2012) reached the same conclusion: most facies span the full range of observed water depths in shallow carbonate environments. These results present stratigraphers with an important question: if shallow carbonate facies are poorly correlated with water depth, how can they record sea level change?
2. **Is meter-scale cyclicity a quantifiable reality or a perceptional artifact?** A second source of skepticism comes from sedimen-

* Corresponding author.
E-mail address: egeyman@alumni.princeton.edu (E.C. Geyman).

https://doi.org/10.1016/j.epsl.2021.116790
0012-821X/

tologists who have sought to quantify the degree of *order* in parasequences—that is, the tendency for facies sequences to follow a characteristic pattern $a \rightarrow b \rightarrow c$. Using Markov-based metrics, Wilkinson et al. (1997) and Manifold et al. (2020) searched for order in carbonate successions that have been deemed cyclic by other stratigraphers. They returned mostly empty-handed, leading Wilkinson et al. (1997) to conclude that meter-scale cyclicity is "perhaps more perceptional artifact than stratigraphic reality."

3. **Is carbonate accumulation dominated by stochastic processes?** A third challenge comes from a statistical point of view. A diverse array of stochastic processes—including earthquakes and radioactive decay—have the properties that (1) the number of events occurring in a finite time interval obey a Poisson distribution, and (2) the waiting times between events follow an exponential distribution (Supplementary Information, section 6). Wilkinson et al. (1999) and Wilkinson and Drummond (2004) (but cf. Burgess and Pollitt, 2012) show that bed transitions and bed thicknesses in modern and ancient carbonate environments possess these same statistical properties, *perhaps* indicating that shallow carbonate deposition is a predominantly random process.
4. **Do parasequences record periodic behavior?** An even trickier statistical observation is that *parasequences*—not just beds—have exponential thickness distributions (Drummond and Wilkinson, 1993a, 1993b). This observation is significant because cycle thickness should scale with cycle duration, since accommodation space is limited by platform subsidence. Thus, it might be hard to reconcile how a periodic forcing could produce cycles with non-modal thickness distributions, leading Drummond and Wilkinson (1993a) to conclude that meter-scale parasequences represent *aperiodic* behavior.
5. **Can we distinguish local from global cycles?** Perhaps the greatest challenge in the interpretation of shallowing-upward parasequences is deciphering whether local shallowing represents internal banktop processes or global sea level change. There are a number of models for the internal generation of repeated shallowing-upward cycles (e.g., Ginsburg, 1971; Burgess, 2001). The classic Ginsburg (1971) model proposes that landward transport of carbonate produced in the subtidal zone fills the inter- and supratidal zones, causing progradation of the shoreline. As the shoreline progrades, the area of the subtidal zone diminishes, reducing carbonate production until eventually subsidence outpaces accumulation. At this point, the platform re-floods, and a new cycle begins. The fact that shallowing-upward parasequences could represent either local or global phenomena adds considerable ambiguity to paleoclimatic interpretations.

Despite the challenges listed above, we remain hopeful that it is possible to extract quantitative sea level histories from carbonate strata for two reasons. First, Dyer et al. (2019) showed that, even if the water depth distributions of different facies overlap (Harris et al., 2015), the information encoded in facies *transitions* and relative thicknesses can be leveraged to create probabilistic records of local water depth change. Second, the pioneering Harris et al. (2015) datasets might be too coarse and poorly-calibrated (with errors of 53% and 66% for the bathymetry and facies maps, respectively—*Supplementary Information,* section 2), to be able to accurately resolve the lateral bathymetric and facies changes giving rise to perceived meter scale parasequences.

We seek to disentangle the relationship between carbonate facies and sea level by:

1. Developing a well-calibrated, high-resolution facies dataset for a test site of the modern Bahamas.
2. Using this facies map and a recently developed bathymetry (Geyman and Maloof, 2019), combined with two new forward modeling approaches, to generate stratigraphic sequences akin to those preserved in the geologic record.
3. Using Hidden Markov Models to test the hypothesis that relative sea level histories can be inferred from the sequences of facies transitions preserved in a stratigraphic column.
4. Exploring whether forced water depth cycles impart characteristic statistical fingerprints in carbonate strata, providing a tool for differentiating between relative sea level cycles generated through internal (unforced) or external (forced) mechanisms.

2. Methods

2.1. Field surveys and generation of the facies and water depth maps

2.1.1. Mapping sedimentary facies

To constrain the facies map, we study 363 point locations in the region NW of Andros Island (Fig. 1b), collecting surface sediment samples for grain size analysis and documenting the bedforms, vegetation, and extent and type of bioturbation. We use a Beckman Coulter LS 13-320 Laser Diffraction Particle Size Analyzer to measure grain size distributions. Next, we apply principal component analysis (PCA) to represent the grain size spectra as linear combinations of just a few characteristic distributions, or principal components (Klovan, 1966). Because we want to create a map of *discrete* facies, we use a k-means unsupervised clustering algorithm to group the grain size data into k clusters. Specifically, we cluster the scores of the first 3 principal components (PCs), but weight each dimension by the percent variance explained by that PC (45%, 34%, and 11% for PCs 1-3, respectively). We let the data determine the optimal number of facies categories by iterating $k = 1$ to 20 and computing the mean intra-cluster variance. As the number of clusters increases, the sediments in each cluster become more similar, and the variance decreases. However, an 'elbow' in the k vs. intra-cluster variance curve occurs at $k = 5$. In other words, after $k = 5$, increasing the number of clusters yields diminishing returns. Thus, we divide the grain size dataset into 5 classes. The grain size clusters broadly align with our field classifications based on the Dunham (1962) scheme, so we will hereafter refer to the classes as mudstone, wackestone, packstone, oolitic grainstone, and shelly grainstone (Fig. 1f-j).

The grain size data provide facies classifications for only 363 point locations. To obtain a continuous facies map, we train a model to predict facies based on intensity values in RapidEye satellite imagery (5 m resolution, Fig. 1b). An important caveat in using optical imagery to classify facies is the fact that image color is controlled by not only bottom substrate (i.e., facies), but also water depth. Since the objective of this study is to explore the relationship between facies and water depth, it is essential that the facies classification remains unbiased with respect to water depth. We therefore transform the RapidEye image to a *depth-invariant* measure of bottom reflectance (Lyzenga, 1978). We apply a convolutional neural network to the depth-invariant bottom reflectance to generate a classified facies map (*Supplementary Information*, section 1.2). Using a held-out set of data not used to train the model, we estimate the overall classification accuracy to be 84% (Fig. 1e).

2.2. Mapping water depth

Geyman and Maloof (2019) created a bathymetry for the region NW of Andros Island (Fig. 1c) based on RapidEye satellite imagery, ~300,000 depth soundings, and a *cluster-based regression* (CBR) algorithm. The CBR algorithm is grounded in the physics of radiative

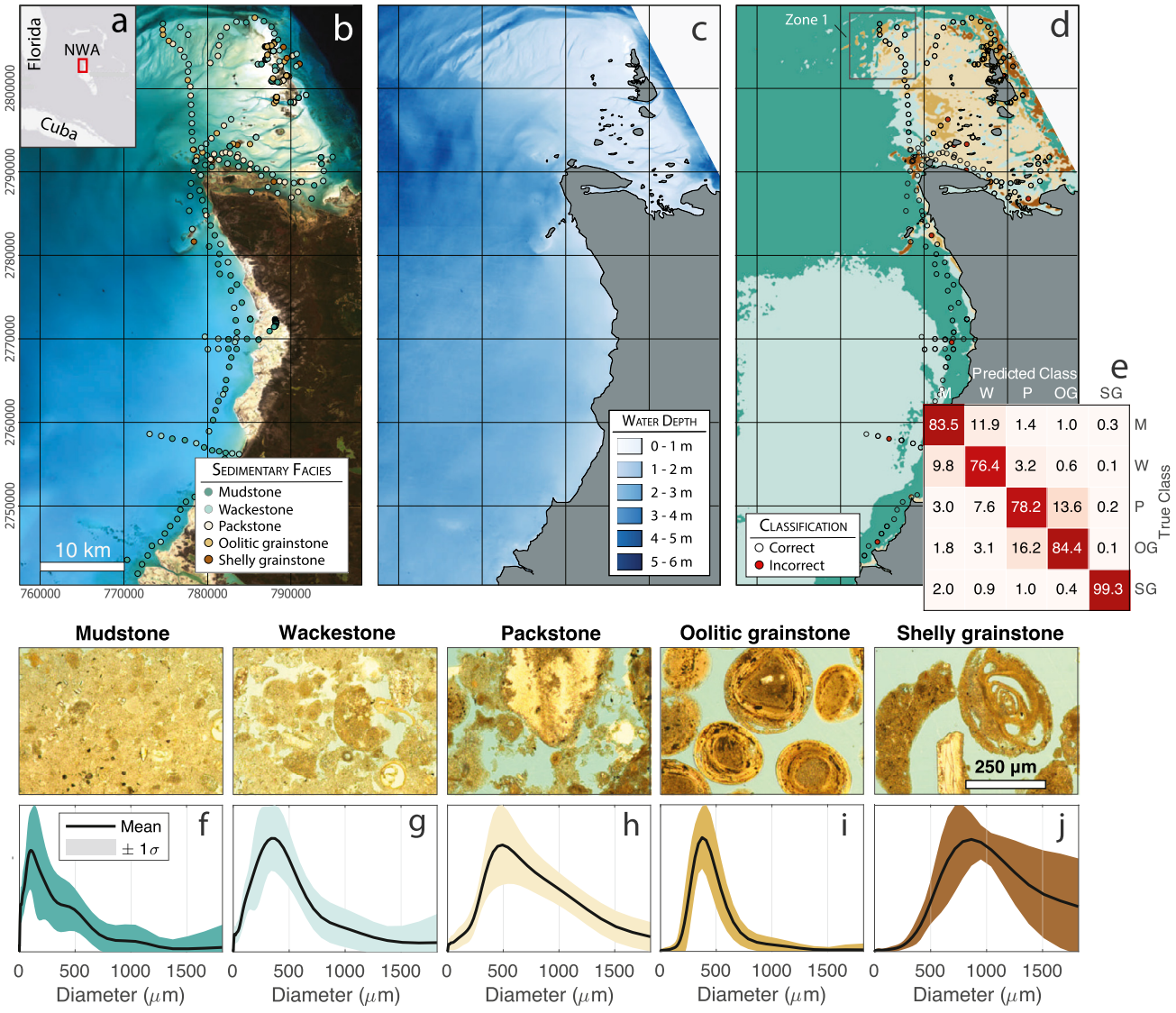

Fig. 1. Sedimentary facies and water depth in the region NW of Andros Island (NWA), Bahamas (a). (b) RapidEye satellite acquisition (March 16, 2018), with the locations of 363 surface sediment samples. (c) Estimated bathymetry, which has a mean absolute error of ~0.19 m (Geyman and Maloof, 2019). (d) Facies map created using the satellite imagery (b) and a convolutional neural network (Mehra and Maloof, 2018) trained with a subset of the surface sediment samples (*Supplementary Information*, section 1.2). (e) The overall accuracy of the facies map is 84%, according to a held-out set of ground-truth data not used to train the model. Much of the classification error results from confusion between either mudstone vs. wackestone or packstone vs. oolitic grainstone. (f-j) Five discrete facies classes determined by an unsupervised clustering of the grain size distributions of 363 sediment samples (*Supplementary Information*, section 1.1). (f) Class 1 (mudstone) is characterized by an abundance of small carbonate particles. (g) Class 2 (wackestone) has a larger mean grain size than class 1, but still has abundant mud (<63 µm). (h) Class 3 (packstone) is poorly-sorted and dominated by larger grains, although it still contains mud. (i) Class 4 (oolitic grainstone) has no mud and consists of well-sorted ooids, peloids, and coated grains. (j) Class 5 (shelly grainstone) has no mud and incorporates a wide range of large grains. (For interpretation of the colors in the figure(s), the reader is referred to the web version of this article.)

transfer in seawater, but made more robust to variable bottom type through the calibration of individual color-to-depth relationships for different spectral classes. The estimated mean error for the final bathymetry is 0.19 m.

2.3. Building stratigraphic sequences from the facies and bathymetry datasets

Beginning in the 1980s, a wave of numerical models sought to reproduce patterns of cyclic sedimentation in shallow carbonates, and to link geological observations to characteristics of ancient sea level (e.g., Read et al., 1986; Koerschner and Read, 1989; Drummond and Dugan, 1999; Goldhammer et al., 1990; Burgess et al., 2001). However, most of these models assume a fully deterministic relationship between water depth and sedimentary facies. Since water depth alone appears to have little predictive power for shallow carbonate facies (Harris et al., 2015), and because we still lack a comprehensive understanding of the other physical/hydrodynamic, geochemical, and ecological controls, we take a different approach than the previous numerical models that inspired this work. Rather than specifying depth-dependent functions of carbonate composition, production, transport, etc. *a priori*, we design two types of *data-driven* forward models, which leverage our observations from the modern Bahamas (Fig. 1) to try to capture how facies and bathymetric variability in a real carbonate environment translate into the stratigraphic record.

2.3.1. Forward model 1: directed vs. random walk

Our first forward model is based on Walther's Law, which postulates that sequential layers in a stratigraphic column represent laterally adjacent facies patches at the time of deposition (Walther, 1894). Imagine a carbonate bank progrades in response to forced sea level fall. We can replicate the vertical sequence of facies deposited during such regression by starting at some

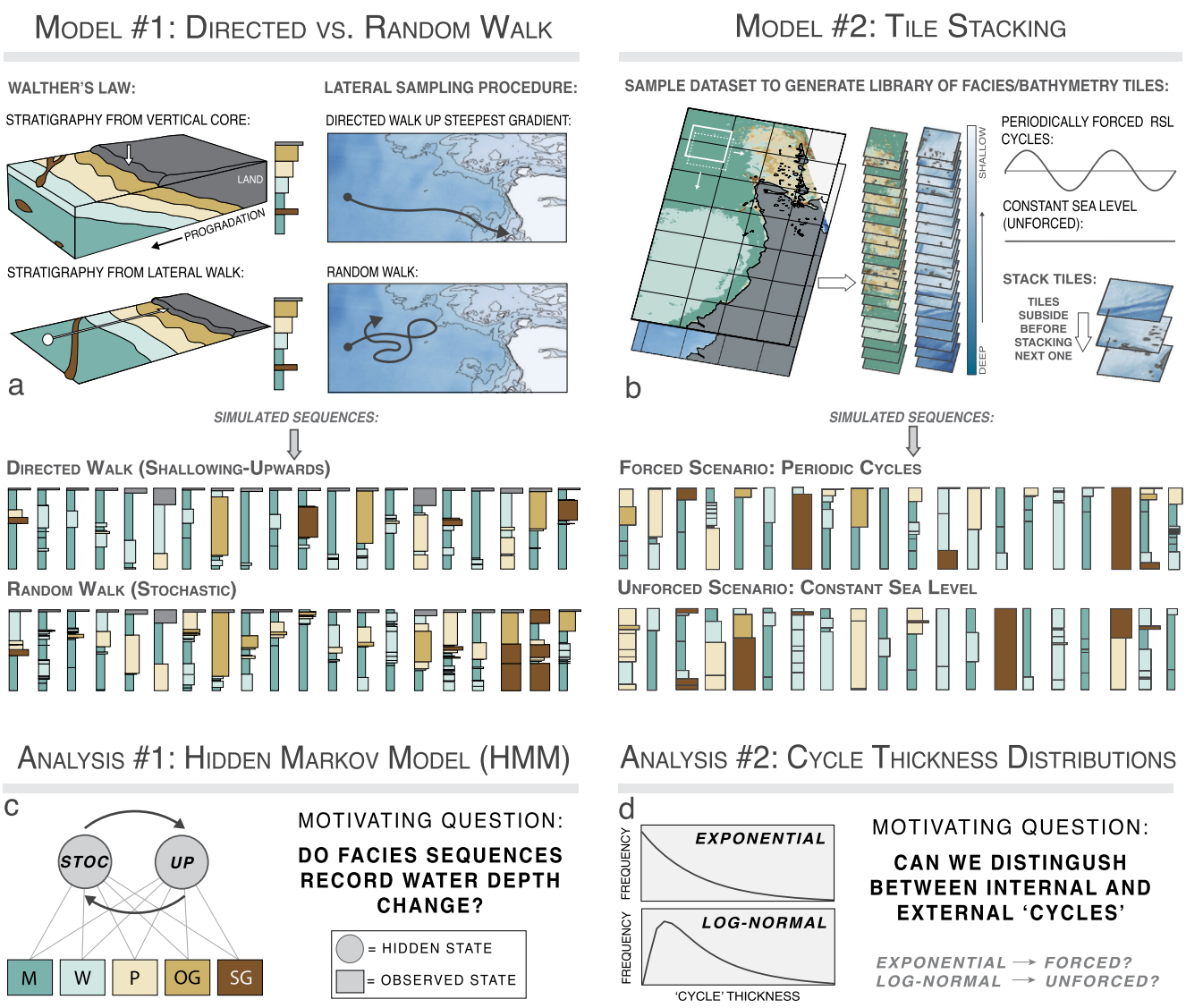

Fig. 2. We use two forward modeling approaches for generating stratigraphic sequences from the facies and bathymetry maps in Fig. 1: (a) the directed vs. random walk model and (b) the tile stacking model. In each forward model, we generate ≥10,000 simulated sequences with different relative sea level histories and forcing conditions. Random samplings of just 20 sequences of each type are shown in the figure. See Fig. 1 for the facies that correspond to each color. Note that these sequences have diverse architecture (e.g., layer thicknesses and facies stacking patterns), and it is difficult to distinguish the different groups of sequences by eye. We analyze the sequences using two approaches: (c) the Hidden Markov Model (HMM), which helps us test the hypothesis that the facies stacking patterns encode relative sea level histories, and (d) analysis of 'cycle' thickness distributions, which helps test the hypothesis that external forcings on relative sea level impart characteristic statistical fingerprints on the preserved strata.

subtidal position on the banktop and walking uphill towards the shoreline, sampling all the facies belts we traverse along the way (Fig. 2a). This translation between space and time is the essence of Walther's Law.

Of course, the stratigraphic record never reflects steady sedimentation, but rather a complex history of deposition, non-deposition, and erosion (e.g., Schumer et al., 2011). As a result, there rarely is a 1:1 correspondence between the lateral distribution of facies and the vertical sequences preserved in the geologic record. In an effort to produce more realistic sedimentary sequences, we track the history of erosion and deposition along each directed walk, building the stratigraphy incrementally and allowing for erosive events (corresponding to bathymetric deepenings along the traverse) to remove some or all of the previous stratigraphy (Fig. 3a).

We generate a library of shallowing-upward parasequences by selecting 10,000 uniformly-distributed random locations across the study area (Fig. 1) and performing directed walks up the steepest average gradient towards land (Fig. 3b). At the same 10,000 initial locations, we create a second set of sequences by performing *random* walks.

While the directed vs. random walk simulation preserves all of the spatial adjacency relationships of facies belts in the Andros map (Fig. 1d), this model allows limited flexibility in specifying different relative sea level histories, and only permits the simulation of a *single* shallowing-upwards parasequence from each initialized location on the banktop. To simulate the stratigraphic response to multiple cycles of forced relative sea level change, we turn to a second kind of data-driven forward model.

2.3.2. Forward model 2: tile stacking

Our tile stacking forward model is designed to capture how modern facies mosaics evolve to stack strata on longer timescales, across numerous relative sea level cycles, and in response to a variety of possible external forcings (Fig. 4). Note that the tile stacking model sacrifices some of the spatial adjacency information captured in the directed vs. random walk model by resampling the Andros dataset into separate tiles. However, like the directed vs.

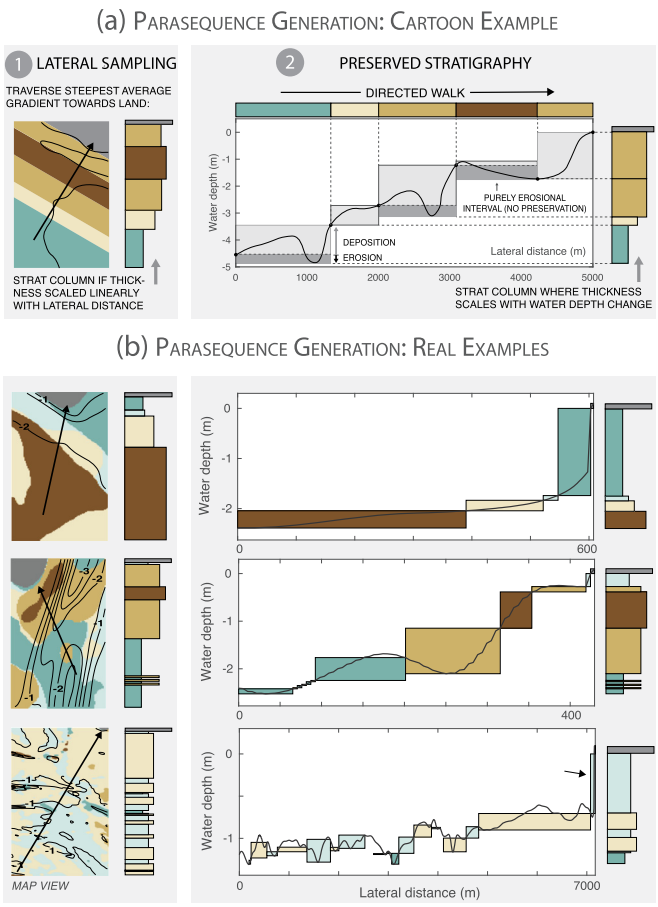

Fig. 3. An illustration of the sampling procedure in the directed vs. random walk model (Fig. 2a). The simplest application of Walther's Law assumes a linear scaling between lateral distance and stratigraphic thickness (Wilkinson et al., 1999; Dyer et al., 2019), as illustrated in panel ①. A more nuanced representation accounts for the role of erosion and topography. In ②, layer thickness records the water depth change within each facies belt along the directed or random walk. Traversing into deeper water represents an erosive event that erases previous stratigraphy. This diagram is inspired by Schumer et al. (2011) and the stratigraphical "staircase" plots of Sadler and Strauss (1990) and others. Note that this way of modeling sedimentation is motivated by the fact that the accommodation space generated through subsidence during the assembly of a single meter-scale parasequence is small (*Supplementary Information,* section 3.1). As a result, the thickness of the stratigraphic column is limited by the water depth at the deepest part of the directed or random walk. Panel (a) shows a cartoon illustration of how we use the water depth along a directed walk to determine the thickness of each sedimentary layer, and (b) shows real examples from the Andros dataset. Notice that there can be a strongly non-linear relationship between the lateral extent of a facies belt and the stratigraphic thickness. Also notice that facies immediately adjacent to land tend to have higher preservation potential, because that is where you find steeper shallowing trends not punctuated by deepening (erosive events). (c) A selection of stochastic and uphill parasequences generated from the directed walks. Note that many landward sequences lack the coarsening-upward character of canonical shallowing-upward parasequences, and that neither group of sequences could be described by a single 'ideal' template.

random walk simulations (Fig. 3), the tile stacking focuses on how temporal variations in seafloor topography control periods of accumulation, nondeposition, and erosion. Although this concept of high-frequency topographic variability exerting a major control on the preserved stratigraphic record is widely recognized (Ganti et al., 2011; Schumer et al., 2011; Straub et al., 2020), it largely has been ignored in previous models of shallow carbonate sedimentation (but cf. Burgess and Wright, 2003).

The tile stacking procedure is outlined in Fig. 4. First, we generate a library of bathymetry and facies tiles ($N = 31,188$) by sampling the Andros datasets in a moving window. Second, we specify a sea level signal, which could be constant (unforced) or oscillatory (forced). For each model timestep, we select a random tile from the set of tiles that have mean water depths within a threshold (e.g., 0.1 m) of the desired sea level for that time step (Fig. 2b). The tile library is sufficiently large that, for each model timestep and desired sea level, there typically are several hundred possible tiles to select from. We let the model grid subside according to the specified subsidence rate, and then stack the newly-selected tile. For each pixel in the model grid, sediment is allowed to accumulate from the elevation of the seafloor in the last timestep to that of the current timestep. When the current seafloor elevation is lower than the last, the sedimentary column is eroded (Fig. 4).

Note that, in the 'unforced' case of the tile stacking model, the local water depth at any given location in the model grid still changes with each timestep due to the random sampling of different bathymetry/facies tiles (Fig. 4). In other words, the movement of facies belts—and the associated water depth changes—modulate erosion, deposition, and different facies ordering patterns in the resulting strata. Such 'unforced' strata, which still can appear qualitatively cyclic and have repetitive shallowing-upwards patterns (Fig. 6g), reflect internal (autogenic) banktop processes, and are akin to the random walk scenario in Fig. 2a. In contrast, the forced tile stacking simulations add increments of water depth change uniformly across the model grid to simulate forced changes in eustasy and/or subsidence on top of the internal banktop dynamics (Fig. 4).

In the simplest model implementation, tiles are selected from a uniform probability distribution over all candidates (those with the appropriate average water depth). In this scenario, a tile that is positioned on the bank near the current tile is not preferentially sampled over a tile from the other side of the map area. In a second implementation of the model—which better incorporates the themes of Walther's Law—more distant candidate tiles are given exponentially smaller sampling weights, encouraging sequential tiles to come from adjacent facies belts. We find that the results discussed in sections 3.2 and 3.3 are robust (insensitive) to these two different model formulations (*Supplementary Information*, section 5). We run the tile stacking forward model with a wide variety of sea level forcings, and explore the model sensitivity to parameters such as the subsidence rate (s), timestep (Δt), tile width (w), cementation time (c), and search distance (λ) (which defines the rate of exponential decay in the probability of selecting increasingly distant tiles). See *Supplementary Information*, section 5, for a discussion of model sensitivity.

2.4. Analysis of simulated stratigraphic sequences

We use the two forward models to probe different questions about how carbonates record sea level. First, the directed vs. random walk sequences allow us to test the hypothesis that facies ordering patterns reliably encode relative sea level histories (Fig. 2c). Second, the tile stacking forward model (Fig. 4) lets us explore whether strata deposited under forced vs. unforced sea level conditions carry different statistical thickness distributions that we could measure in the geological record.

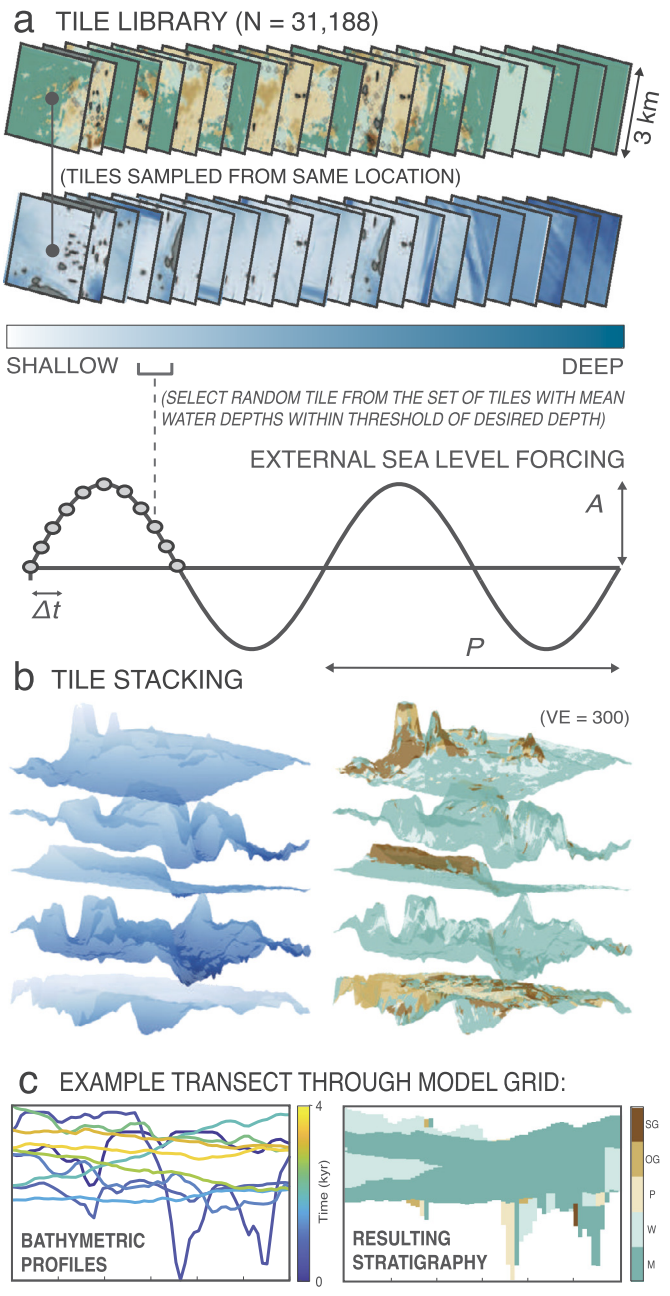

Fig. 4. An overview of the tile stacking forward model. After generating the tile library (a) by resampling the Andros facies and bathymetry dataset in a moving window (Fig. 2b), we specify an external sea level forcing, which could be oscillatory, as shown in (a), or constant (unforced). (b) For each model timestep, we select a random tile from the set of tiles that have a mean water depth within a narrow range of the desired sea level for that time step. (b) The selected tile is stacked onto the model grid, which has subsided $\Delta z = s \times \Delta t$ since the last timestep, where s is the subsidence rate and Δt is the timestep duration. On average, there will be net deposition in the model grid of thickness Δz per model timestep, but the topographic variability across each tile (on the order of meters) greatly outweighs the long-term accommodation generation through subsidence (on the order of mm to cm per model timestep), causing spatially-variable deposition and erosion. (c) Simple transects across the 3D model grid. With time, the bathymetric profiles—which represent the position of the seafloor—migrate upward relative to the base of the subsiding platform, leading to preservation of strata. But at any given timestep, half or more of the model grid can experience erosion.

2.4.1. Hidden Markov Model (HMM)

Markov chain analysis has been applied to carbonate strata for decades (e.g., Wilkinson et al., 1997; Lehrmann and Goldhammer, 1999; Burgess, 2016; Manifold et al., 2020). Traditional Markov analysis involves tabulating all the first- or second-order facies transitions from a stratigraphic sequence into a transition matrix like the one in Fig. 5b. When a stratigraphic sequence has a high degree of Markovian *order* (e.g., facies *A* typically is followed by facies *B*), the transition probabilities are concentrated in just a few elements of the transition matrix (Wilkinson et al., 1997). Whether the observed degree of Markovian order in a particular stratigraphic section is statistically significant can be assessed by randomly reshuffling the stratigraphic sequence *n* times and comparing the transition matrices from the observed section with those from the reshuffled sections (e.g., Burgess, 2016).

At least implicitly, Markov chain analysis is built on the notion of an 'ideal cycle' (or a small collection of such cycles). If facies *A* typically is followed by facies *B*, which is followed by facies *C*, then $A \rightarrow B \rightarrow C$ represents the ideal cycle. Burgess (2016) illustrates a nice method for identifying such cycles from sedimentary sequences. However, we find that traditional Markov analysis and notions of the 'ideal cycle' are ineffective when applied to the directed vs. random walk sequences (*Supplementary Information,* section 7). The complexity of shallow carbonate environments appears to prohibit characterization of relative sea level change from a handful of patterns or templates. Moreover, the diversity of stratigraphic architecture makes it difficult to distinguish uphill (directed walk) vs. stochastic (random walk) sequences. Consider the example sequences in Fig. 3c. In the geological record, the stochastic sequences capped by subaerial exposure surfaces may be mis-identified as representing sea level fall, while real shallowing might be overlooked in the uphill sequences lacking the canonical coarsening-upward character. Can we build a predictive model to see signal through the noise and reliably decode quantitative sea level histories from carbonate strata? Dyer et al. (2019) demonstrate that Hidden Markov Models (HMMs) are an effective way to translate facies sequences to probabilistic inferences of water depth change, even when individual facies are poor predictors of local water depth.

The HMM is a tool designed to uncover hidden variables that cannot be observed directly (e.g., ancient sea level change), but that control the sequence of variables that can be observed (e.g., sequences of facies in the geologic record) (Rabiner and Juang, 1986). The innovation of the HMM over a traditional Markov model is that the HMM can draw from *multiple* transition matrices (one for each hidden state), thereby allowing extra degrees of freedom to accommodate cycles that are less 'ideal.'

As a simple example of an HMM, imagine someone stands behind a curtain, flipping either a fair or a biased coin. All we observe is the sequence of heads/tails, and our goal is to predict whether the coin is fair at any given time. The coin—biased or fair—represents the *hidden state*. By specifying the *emission probabilities* (the probabilities with which biased and fair coins produce heads) and the *state transition probabilities* (the probability of swapping the biased and fair coins), we can create an HMM to estimate the probability that, at any given timestep, the fair coin is being used and consequently the probability that the next coin flip will produce heads (Fig. 5a; Rabiner and Juang, 1986).

The framework for applying an HMM to stratigraphic sequences is exactly analogous to the coin example (Fig. 5a). The hidden state is the sea level regime: relative sea level fall or stochasticity. We explicitly test relative sea level fall (and not rise), since parasequences recording relative sea level fall are thought to dominate the thickness of most cyclic stratigraphic records (Bosence et al., 2000; Grotzinger, 1986; Goldhammer et al., 1990; Read et al., 1986; Fischer, 1964). If carbonate facies are a real but noisy recorder of water depth, certain sequences of facies should be more probable under the relative sea level fall state than the stochastic (random walk) state.

2.4.2. Analyzing thickness distributions of sedimentary layers and 'cycles'

We analyze the strata from the tile stacking model with the goal of identifying simple statistical metrics that differentiate between strata deposited under external sea level forcing vs. those that only experience internal platformal variability. In particular, we are interested in investigating the thickness distributions of sedimentary cycles to address the question from section 1 about whether periodic forcings can generate parasequences with exponentially-distributed thicknesses (Drummond and Wilkinson, 1993a, 1993b). While the cycles analyzed in Drummond and Wilkinson (1993a, 1993b) typically are interpreted as shallowing-upwards sequences, we note that the ambiguity of facies to water depth transfer functions (i.e., the overlapping water depth distributions of each facies) means that a stratigrapher could not identify deterministically individual shallowing-upward cycles in Bahamian carbonates. Consider the diversity of stratigraphic architecture in Fig. 3c for an example of how challenging identifying true shallowing-upward cycles would be. Therefore, in the analysis of the tile stacking strata, we rely on simple but objective criteria for identifying meter-scale sedimentary cycles. The first rule-based system uses the depth rank of the facies in our map area (i.e., mudstone > wackestone > shelly grainstone > oolitic grainstone > packstone—Fig. 10a). Since this first rule-based system relies on *a priori* knowledge of the average water depths of each facies (knowledge that is impossible to acquire for ancient strata), we also use a second system that defines sedimentary cycles as runs of coarsening-upwards facies. Neither system accurately captures local shallowing-upwards sequences, but these rule-based criteria provide a simple way to group facies sequences into individual 'cycles' and ultimately help us diagnose whether strata formed under the influence of forced relative sea level cycles.

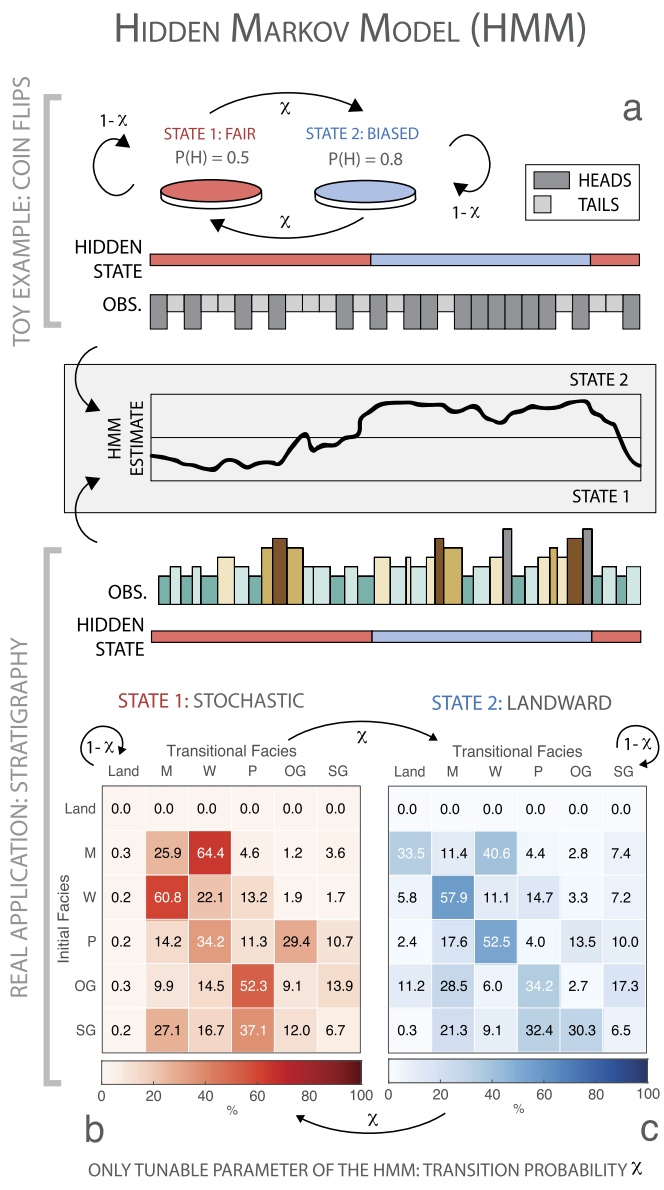

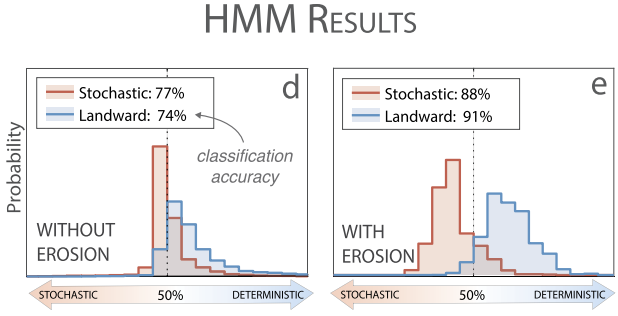

3. Results and discussion

3.1. HMM: results from the directed vs. random walk simulation

We compute the facies transition probabilities—the primary HMM input—by counting transitions in the 10,000 landward and stochastic sequences (Fig. 5b-c). Unsurprisingly, the transition from any facies to land (i.e., a subaerial exposure surface in the stratigraphic record) is much more common in landward than stochastic sequences. The transition from mudstone to land is particularly diagnostic of shallowing (Fig. 5b-c).

Next, we apply the trained HMM to our directed vs. random walk sequences. Note that in Fig. 3b, we model stratigraphy in two ways. Panel ① gives a strict Walther's Law interpretation, where the lateral facies extent directly translates into vertical thickness in a stratigraphic column (Wilkinson et al., 1999; Dyer et al., 2019). Panel ② accounts for variable deposition and erosion along the traverse, as determined by local topography (Schumer et al., 2011). Panel ② represents a more realistic depiction of meter-scale stratigraphy, and also yields better classification results (Fig. 5e). The HMM can distinguish between landward and stochastic stratigraphic sequences with ~90% accuracy. In other

Fig. 5. (a) Using an HMM to identify a decrease in water depth from a sequence of carbonate facies is analogous to using an HMM to determine whether someone is flipping a biased coin based on a sequence of heads/tails. An HMM consists of just two elements: (1) a matrix that describes the probability of each *observed* state (e.g., heads or tails) given the current *hidden* state (e.g., biased or fair coin), and (2) the probabilities of jumping from one hidden state to another. In the application of the HMM to sea level inference, (1) is empirically determined from the facies transition frequencies in the collection of 10,000 synthetic landward and stochastic sequences (b-c), so the only tunable parameter in the model is χ, the probability that the hidden state changes in any given stratigraphic layer. We determine χ through a standard hyperparameter optimization procedure, and find that the final results are relatively insensitive to χ (*Supplementary Information*, section 3.3). Note in (b-c) that the transition probabilities are computed from the synthetic stratigraphic sequences that include the effects of erosion/topography (Fig. 3b, ②). Analogous transition matrices from Fig. 3b, ① are provided in *Supplementary Information*, section 4. (d-e) HMM-derived shallowing probabilities for the 10,000 stochastic and landward facies sequences, both without (d) and with (e) the effects of erosion (Fig. 3). A perfect model would produce non-overlapping distributions where all stochastic sequences are assigned shallowing probabilities <50% and all landward sequences are assigned shallowing probabilities >50%.

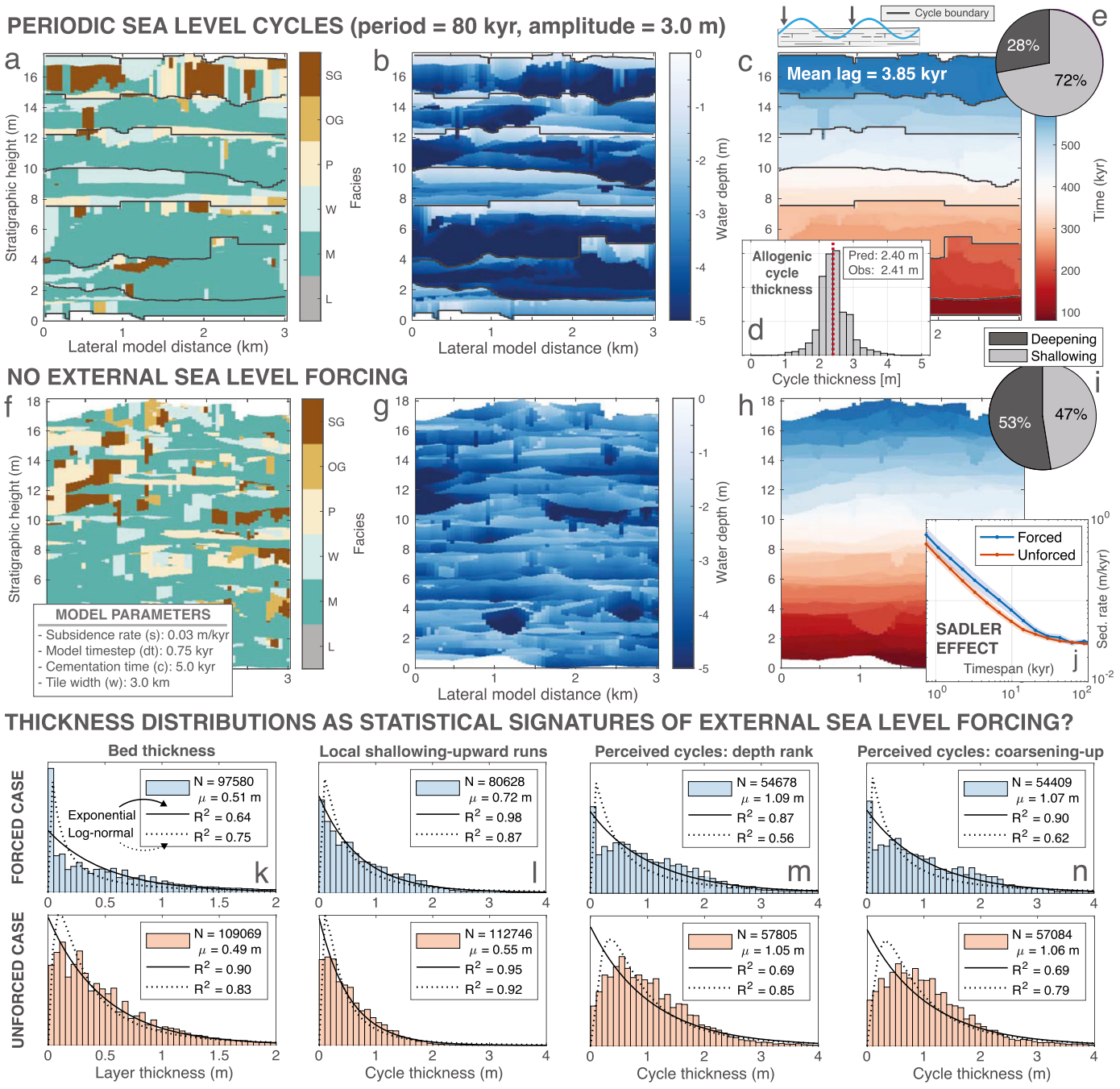

Fig. 6. Example results—(a, f) sedimentary facies, (b, g) local water depth, and (c, h) time of deposition—for 2D cross sections of tile stacking model runs (Fig. 4) with oscillatory vs. constant sea level. (c) The mean lag—defined as the time between platform flooding and when the first sediments in the stratigraphic column were deposited—is 3.85 kyr in this particular simulation, although the lag depends on parameters including the period and amplitude of sea level forcing, the subsidence rate, and the model timestep. (d) As expected, the thickness of sediment deposited between each sea level cycle is tightly-distributed around a mean value equal to the period × subsidence rate. (e, i) In the simulation with periodic sea level cycles, 72% of facies transitions involve a reduction in local water depth (i.e., shallowing) (e), while in the simulation with constant sea level, only ~50% of facies transitions involve shallowing (i). (j) The simulated stratigraphy for both model runs displays the Sadler effect, where measured sedimentation rate decreases as a power law function with increasing timespan (Sadler, 1981). (k-n) A comparison between the thickness distributions of layers (k), true shallowing-upward cycles (l), and *perceived* shallowing-upward cycles (m-n) in the oscillatory (forced) and constant (unforced) sea level regimes. The local shallowing-upward runs (l) are defined as runs of continuous decrease in the depositional water depth. Since the true depositional water depth cannot be determined directly from the geologic record, the 'perceived' cycles (m-n) represent simple rule-based interpretations of shallowing from the stratigraphy. In (m), the cycles are based on the depth rank of facies in our map area (Fig. 10a). In (n), cycles are determined using the simple assumption that coarser facies occupy shallower water.

words, we can reliably detect shallowing based on quantitative analysis of diverse and visually random (Fig. 3c) facies sequences. However, the HMM is unable to distinguish between shallowing caused by external forcing versus internal processes (e.g., Ginsburg, 1971). To understand how an external sea level forcing affects patterns of carbonate sedimentation, we turn to the tile stacking model.

3.2. Tile stacking model: reproducing classical observations

Fig. 6 shows the results of two tile stacking simulations with the same parameters but oscillatory vs. constant sea level forcing. In Fig. 6—and in all other model runs—we find that the forward model reproduces a number of classical observations of carbonate sedimentology. For example:

1. **Shallowing-upward motifs are ubiquitous**. Both forced and unforced simulations produce abundant shallowing-upwards sequences (Fig. 6). This tendency for shallowing-upward motifs is readily understood by the fact that bathymetric deepenings—for example, from tidal channels—will erode previously-deposited sediments, creating extra accommodation space for sediments to fill (shallowing-upward), before the next local bathymetric deepening incises the stratigraphy and initiates the next shallowing-upward sequence. Note that this process does not require external sea level change. However, one result of the tile stacking model is that a higher proportion of facies transitions represent shallowing in the externally-forced scenario (Fig. 6e) than in the unforced scenario (Fig. 6i).
2. **Lag arises naturally.** A canonical shallowing-upward parasequence begins with deeper-water facies that lay directly (and often disconformably) above the shallow facies capping the previous cycle. The abrupt transition from 'shallow' to 'deep' facies is somewhat difficult to explain considering that measured rates of sediment production in Holocene platform environments are an order of magnitude (or more) faster than long-term accommodation generation (Schlager, 1981). In other words, if carbonate production easily can keep pace with subsidence, why wouldn't the available accommodation space continuously be filled by shallow facies? In order to reproduce the geologic observation of abrupt shallow-to-deep transitions at cycle boundaries, most forward models impose a pre-defined *lag parameter*, mandating that the platform subsides to a certain depth or for a certain amount of time before sedimentation can resume (e.g., Read et al., 1986; Koerschner and Read, 1989; Drummond and Wilkinson, 1993b; Goldhammer et al., 1990). But such a parameterization sheds no light on the *origins* of the lag phenomenon. Tipper (1997) was able to produce lag, but only by assuming that the slow recolonization by carbonate-producing organisms on the bank following immersion is the cause of lag. In contrast, lag—which we define as the time between when the platform is flooded and when the first sedimentary layer is preserved (Ginsburg, 1971; Grotzinger, 1986; Tipper, 1997)—is a natural result of our tile stacking model. Although the exact duration of the lag is sensitive to parameters such as subsidence rate and the period of sea level oscillation (*Supplementary Information*, section 5.2), lag is a common feature of all simulations, and can be understood as the simple result of erosion (e.g., Burgess and Wright, 2003). Imagine the survivorship of a parcel of sediment deposited when the platform is first flooded. The random fluctuations in seafloor topography (modeled as the repeated selection of bathymetric tiles—Fig. 4) mean that this parcel of sediment is less likely to persist in timestep $(t+1)$ after platform flooding, and even less likely to persist in timestep $(t+2)$, etc. In the final stratigraphy, a cycle's first preserved sedimentary layer likely will have been deposited some duration $\Delta t > 0$ after flooding.
3. **Sedimentation patterns obey the Sadler effect.** Another result of the decaying survivorship of a parcel of sediment with time is the temporal 'incompleteness' of the stratigraphic record, and the time-dependence of such incompleteness (e.g., Sadler and Strauss, 1990; Straub et al., 2020). Sadler (1981) demonstrated that, as a result of stratigraphic incompleteness, thinner stratigraphic sections record faster average accumulation rates. For example, while an individual sedimentary layer may be deposited in just hours or days, a stack of *two* layers might represent thousands or even millions of years, due to periods of non-deposition and erosion between the layers. More quantitatively, Sadler (1981) showed that stratigraphic timespan vs. sedimentation rate obeys a power law. We observe power law behavior ('Sadler effect') in both the forced and unforced scenarios (Fig. 6j), matching the observations that Sadler (1981) made from diverse stratigraphic data.
4. **Bed thicknesses are well-described by exponential distributions.** As Wilkinson et al. (1999) and Drummond and Wilkinson (1996) point out (but cf. Burgess, 2008), bed thicknesses in carbonate successions in the geologic record have the property that, for most of the population, frequency drops off exponentially with linearly-increasing size. Whether such distributions are better-described as exponential or lognormal depends on whether the thinnest beds are the most abundant, a subtlety that is highly-sensitive to the stratigrapher's tendency to lump together very small beds (Fig. 9h-i). Our forward model, which does not suffer the bias of geologists skipping the thinnest layers when translating outcrop to a stratigraphic log, reproduces the observations that bed thickness distributions are exponential (Fig. 6j). This exponential behavior is a logical result of the model formulation. In the context of our tile stacking model, a thick bed means that, after a pile of sediment was deposited, local water depth remained shallow (non-erosive) for many subsequent timesteps, such that the layer was advected downward through subsidence until it was protected from erosion (Fig. 4). Consider again a coin-toss analog, where heads represent local bathymetric deepening and tails represent local shallowing. Obtaining a thick bed requires getting many subsequent tails; the longer the string of tails, the thicker the sedimentary layer. Since runs of consecutive tails are exponentially-distributed, so too are layer thicknesses.

3.3. Model implications: cycle thickness distributions as robust indicators of sea level forcing?

Encouraged by the fact that the tile stacking model naturally reproduces several aspects of real carbonate stratigraphy (section 3.2), we use the model to explore sedimentation patterns in response to a wide range of internally and externally forced scenarios. We iterate through different subsidence rates, model timesteps, period and amplitude of sea level forcing, etc., in order to identify potential patterns in carbonate stratigraphy that might be diagnostic of the external sea level forcing (i.e., oscillatory vs. constant).

We focus on low-amplitude external sea level cycles (e.g., $\leq$5 m) because (1) these cycles are harder to unambiguously identify in stratigraphic sequences than Pleistocene-style $\sim$100 m sea level variability, and (2) these cycles are more likely to dominate greenhouse periods (which constitute the majority of the geologic record), when thermosteric effects and/or small glaciers and ice caps only contribute a few meters to global sea level change. Additionally, during periods of high-amplitude glacioeustasy, parasequences only form during the brief window when the bank is submerged. For example, the GBB has been underwater for $\sim$10% of the last (Eemian-Holocene) sea level cycle (e.g., Medina-Elizalde, 2013). During this submerged interval, the behavior we capture in the forward model—for example, how banktop topographic variability drives repeated shallowing-upwards motifs and exponentially-distributed layer thicknesses—describes sediment packages deposited during high-amplitude eustasy just as well as those deposited during low-amplitude eustasy.

In the literature, subaerial exposure surfaces often are interpreted as unambiguous evidence for sea-level fall (e.g., Strasser (1991), Burgess (2001), although see Burgess et al. (2001) for a model of how lateral sediment transport can create supratidal islands in the absence of eustasy). In our synthetic stratigraphy (created through both the directed vs. random walk and the tile stacking models—Fig. 2), subaerial exposure surfaces abound in stochastic/unforced scenarios. Land-capped stochastic sequences in Fig. 3c represent cases in which the random walk intersected

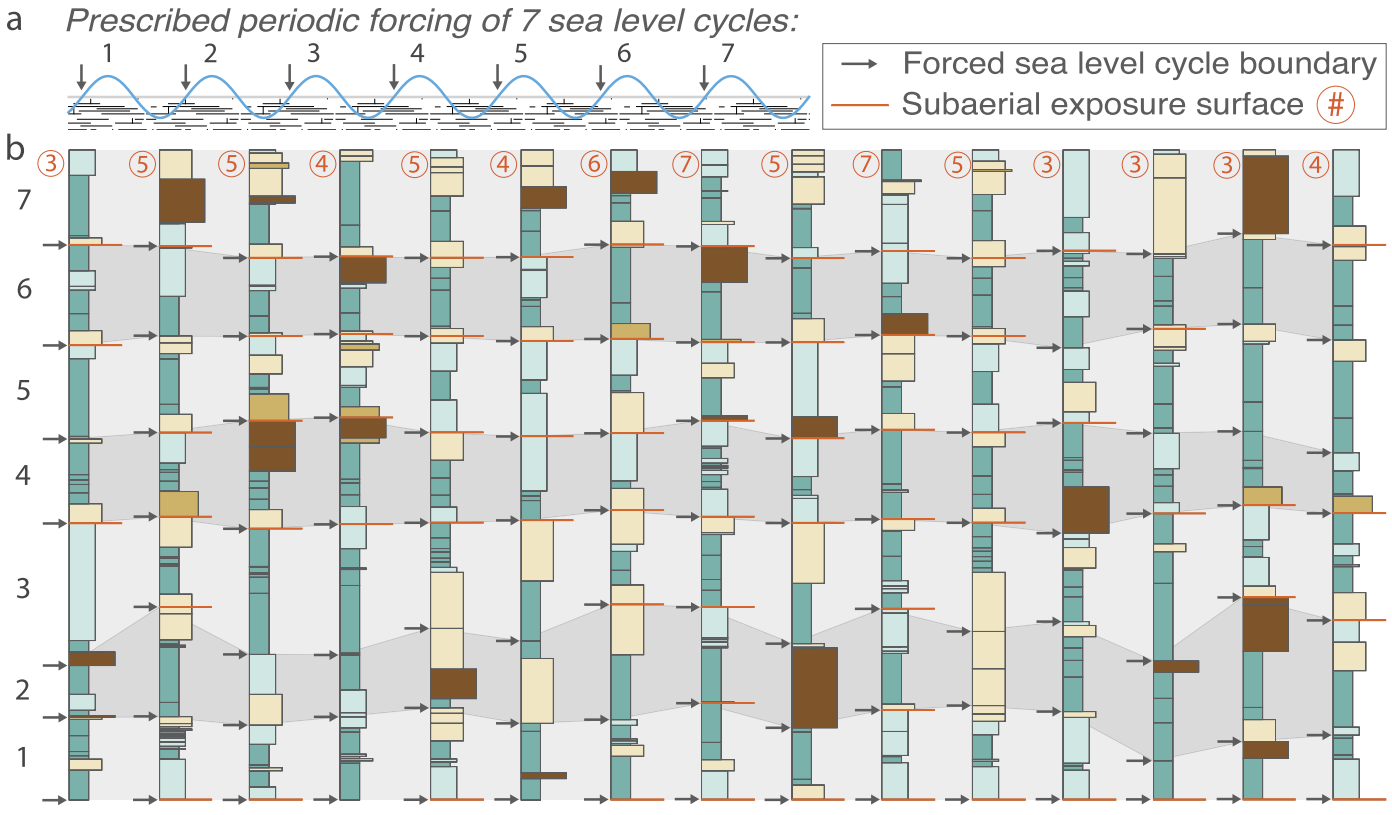

Fig. 7. Fifteen example stratigraphic columns from the forward model run in Fig. 6a-c (forced scenario). The cartoon in the upper left shows where cycle boundaries (7 total) are defined relative to the sinusoidal forcing. For a time window of 0.75 kyr, 93-96% of the total time is missing in the columns above, illustrating the incompleteness of the stratigraphic record. Additionally, although not part of a real geographic cross section, these modeled stratigraphic columns are time-correlative. It would be difficult to link the sections using classical lithostratigraphic correlation—even matching subaerial exposure surfaces would prove challenging, since the number of subaerial exposure surfaces varies from 3 to 7 (although note that Pleistocene-style ~100 m sea level oscillations would generate subaerial exposure surfaces at every boundary, in contrast to the low-amplitude eustatic cycles modeled here). This set of stratigraphic columns illustrates the diversity of facies architectures and stacking patterns exhibited across short ($\leq$3 km) lateral distances in response to the same eustatic forcing, and demonstrates the need for modeling and statistical tools (such as HMM and distributional analysis) that see through the noise of natural intra-shelf variability to extract information about the sea level regime.

land. Likewise, in the tile stacking model, subaerial exposure occurs in unforced simulations when portions of the model tiles lie above sea level (i.e., islands and shoals). Finally, for the strata deposited under externally forced oscillations in sea level (Fig. 6a-c), many true cycle boundaries are *missing* subaerial exposure surfaces, because those surfaces have been removed by subsequent erosion (Fig. 7). While identifying eustatic cycles directly from strata would be very useful, the diversity of stratigraphic architectures and the non-uniqueness of subaerial exposure surfaces makes this task challenging. We seek new ways of inferring externally forced sea level oscillations based on quantitative patterns derived from stratigraphic data.

We observe that the thickness distributions of *perceived* cycles (defined by simple rule systems based on depth rank or coarsening-upward facies—section 2.4.2) are better described by exponential functions when the external sea level forcing is oscillatory, and better described by lognormal functions when sea level is constant (Fig. 8b-c). This result remains consistent across model runs, regardless of the choice of model parameters. We postulate that the unforced scenario leads to lognormal distributions because the constant sea level spreads sedimentation equally across the entire time window, allowing the frequency of deepening events to reach a characteristic timescale, which corresponds to the mode in the lognormal distribution (Fig. 2d) and is a function of the rate at which facies patches migrate across the platform (parameterized as Δt in our numerical model implementation). In contrast, the forced scenario leads to exponential distributions because sedimentation is localized to brief windows of time—(1) when the platform is first flooded, and (2) during sea level fall right before the banktop is exposed (*Supplementary Information*, Figs. 16–17). Squeezing sedimentation into these short time intervals prohibits cycles from equilibrating to a characteristic thickness, preventing the generation of a modal thickness > 0 and supporting cycle thickness distributions that are better described by decaying exponential functions (Fig. 2d).

It is perhaps surprising that forced and unforced scenarios cannot be distinguished using the thicknesses of local depositional water depth cycles (Fig. 8a), even though they are so effectively separated using the thicknesses of cycles inferred from facies ordering (Fig. 8b-c). Natural topographic variability on the banktop drives high-frequency changes in local water depth unrelated to the sea level forcing (*Supplementary Information*, Figs. 16–17). Using facies sequences to define cycles—while imperfect because of the lack of a 1:1 correspondence between facies and water depth—seems to act as a sort of low-pass filter to remove the exponential noise of topography and better differentiate patterns of accumulation under forced and unforced sea level regimes.

Since the perceived shallowing-upward cycles are based on straightforward rule systems, the implication is that anyone could measure a detailed stratigraphic section from a shallow carbonate sequence, tabulate the cycle thickness distributions, and make an inference about whether such sediments were deposited under constant or oscillatory global sea level. The result in Fig. 8b-c represents a hypothesis that we can test with detailed observations from the geologic record. As a first example, we consider a section of well-exposed shallow water carbonates deposited in the

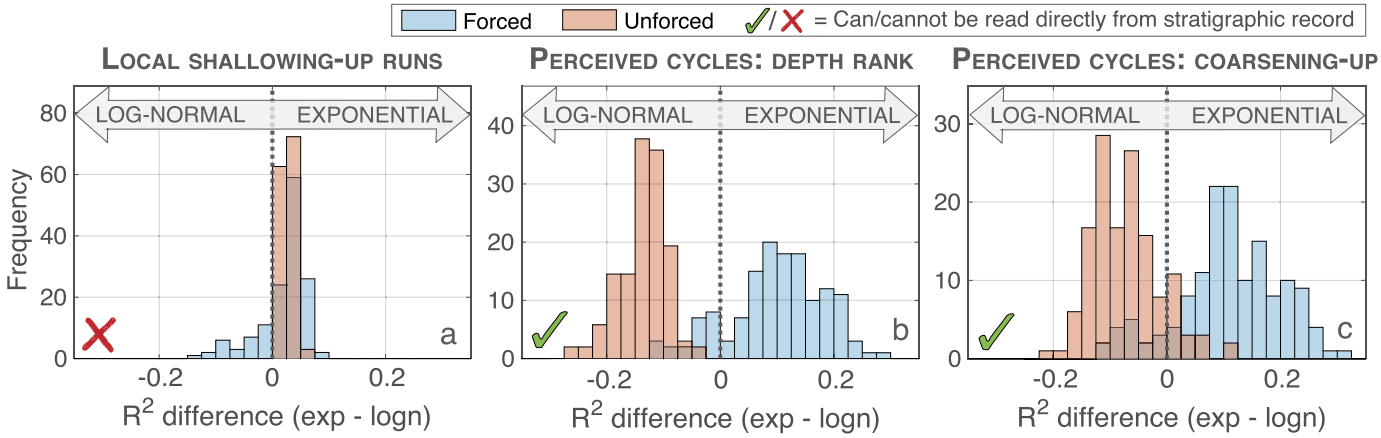

Fig. 8. Over 140 runs of the forward model with different parameters (*Supplementary Information*, section 5.2) show consistent trends in the thickness distributions of (a) local runs of decreasing depositional water depth, and (b-c) perceived shallowing-upward cycles. The *x*-axis displays the difference in the R^2 value between exponential and lognormal fits to the thickness distributions; positive values indicate distributions that are more exponential and negative values indicate distributions that are more lognormal. (a) The local shallowing-upward runs are approximately equally well-described by lognormal and exponential distributions. Note, however, that you cannot glean (a) from the geological record. (b-c) *Perceived* shallowing-upward cycles based on simple facies ordering rules appear to be diagnostic of the sea level forcing; oscillatory sea level produces more exponential distributions and constant sea level produces more lognormal distributions.

midst of the Late Paleozoic Ice Age (LPIA), a period when extensive glacioeustasy has been inferred from both near- and far-field records (e.g., Montañez and Poulsen, 2013).

3.4. Geologic example: sea level forcing during the mid-Carboniferous

The LPIA (330-260 Ma) is thought to be a dynamic interval characterized by periods of waxing and waning ice sheets, as well as periods of either ice stability or relatively ice-free conditions (Montañez and Poulsen, 2013; Bishop et al., 2010). Attempts at inferring sea level from parasequence architecture, coastal onlap, and erosional relief (e.g., Ross and Ross, 1987; Veevers and Powell, 1987; Bishop et al., 2010) suggest a local minimum in the magnitude of sea level oscillations in the middle of the LPIA during the Atokan stage (~315 Ma, Fig. 9). The hypothesis, based on inferences from our tile stacking model, is that the increasing sea level variability coming out of the Atokan should correspond to a shift in the thickness distributions of perceived shallowing-upward cycles from lognormal to exponential (Fig. 8). To test this hypothesis, we measure a detailed stratigraphic section in the exceptionally-exposed shallow carbonates of the Bird Springs Formation in Arrow Canyon, Nevada (Fig. 9). We take care to document every single layer ($n = 696$) at the cm-scale to minimize bias in bed thickness-frequency distributions (Drummond and Wilkinson, 1996; Fig. 9h-i), although we note that this task is inherently a qualitative one that can vary between stratigraphers (Pollitt et al., 2015). We find that the thickness distributions of perceived cycles become increasingly exponential in character across the Atokan, which is consistent with the inferences of increased glacioeustasy based on sequence-stratigraphic arguments (Ross and Ross, 1987; Veevers and Powell, 1987).

3.5. Revisiting challenges to the parasequence paradigm

Our observations from the modern Bahamas, coupled with two new data-driven methods for simulating stratigraphic sequences, allow us to revisit some of the questions posed in section 1.

1. **Are facies reliable recorders of water depth?** Our facies map of NW Andros (Fig. 1d) suggests a somewhat tighter coupling between facies and water depth (Fig. 10a) than suggested by Harris et al. (2015), Purkis et al. (2012, 2014), and Rankey (2004). For example, the mudstone distribution only overlaps with the packstone and oolitic grainstone distributions by 4% and 3%, respectively (Fig. 10a). However, note that the water depth distributions of each facies observed in map view at any given snapshot in time do not necessarily reflect the depth distributions of facies preserved in the stratigraphic record. For example, recall in the directed vs. random walk simulation how the lateral extent of each facies belt was decoupled from thickness in the stratigraphic column (Fig. 3), since large facies belts in low-gradient regions led to thin sedimentary layers, and bathymetric deepenings (erosive events) removed the stratigraphic record of some facies belts altogether.
   The water depth distributions extracted from our simulated stratigraphic sequences (Fig. 10b-c) suggest a *less* deterministic relationship between facies and water depth than observed in map view. Nevertheless, building on the work of Dyer et al. (2019), we show that, even if the water depth distributions of each facies are overlapping, carbonates reliably encode water depth change through facies *transitions* (Fig. 5e).
2. **Is meter-scale cyclicity a quantifiable reality or a perceptional artifact?** The diversity of facies architectures in Bahamian shallowing-upward parasequences (Fig. 3c) helps to explain why previous attempts to identify order through the 'ideal cycle' (e.g., Burgess, 2016; Manifold et al., 2020) are not always fruitful (*Supplementary Information*, section 7). Our results suggest that the HMM framework is more robust to natural variability in carbonate environments than simpler Markov-based metrics (Burgess, 2016; Wilkinson et al., 1997).
3. **Is carbonate accumulation dominated by stochastic processes?** We use our new facies map (Fig. 1d) and the stratigraphic sequences derived from it (Fig. 3c) to determine whether Bahamian carbonates have scaling relationships consistent with stochastic processes. The theoretical Poisson-distributed facies areas and exponentially-distributed bed thicknesses proposed by Wilkinson et al. (1999) represent exceptional matches to our observations (R^2=0.99, *Supplementary Information*, section 6). Meanwhile, our ability to distinguish stochastic from shallowing-upward sequences (Fig. 5e) disproves the notion that carbonate sequences are truly random. We take the view that sedimentation represents a largely stochastic process (influenced by storm events, channel avulsion, etc.), which leads to the statistical distributions consistent with random processes. However, successful HMM classification (~90% accuracy) implies that sedimentary facies must be real—albeit noisy—recorders of water depth.

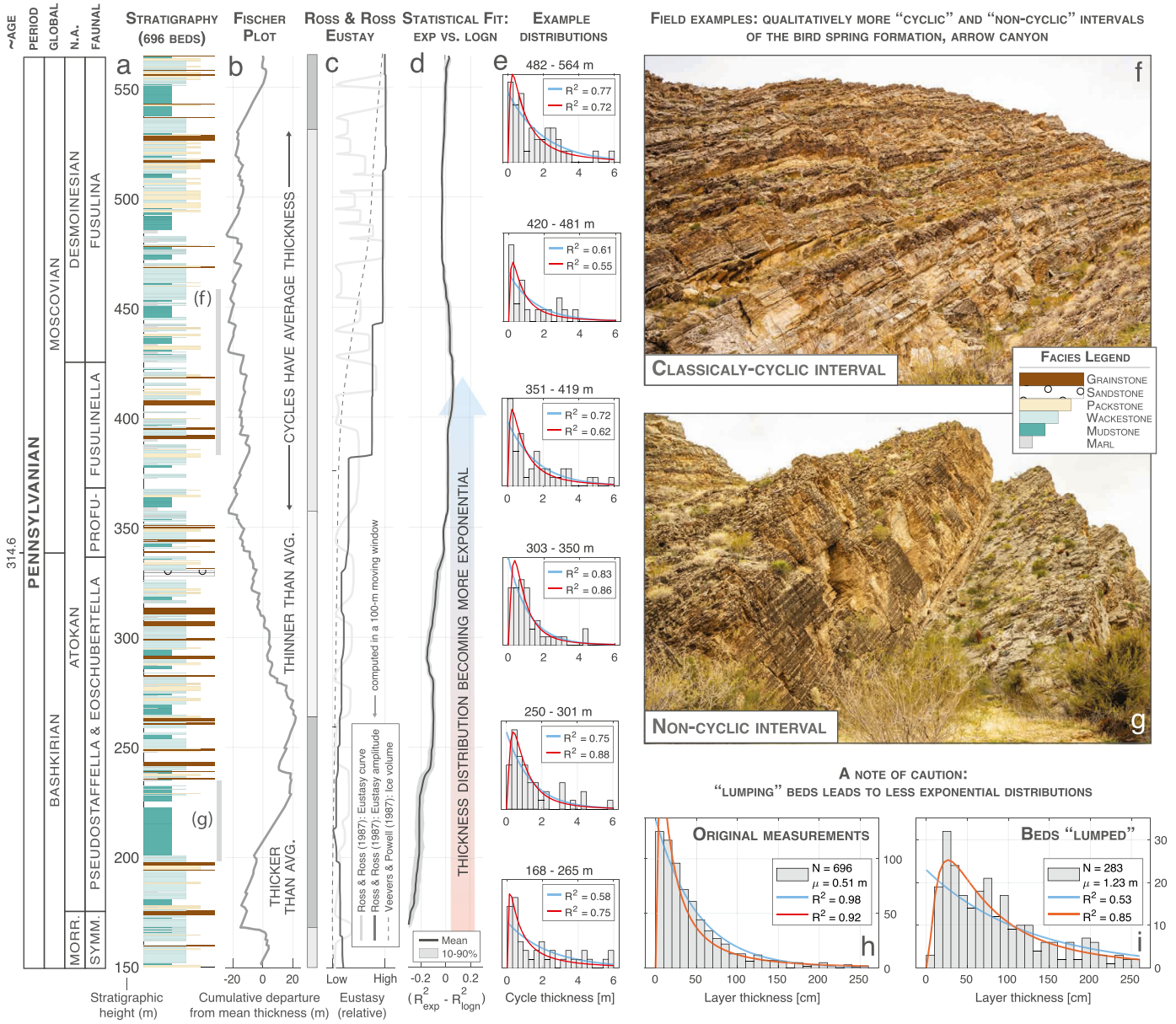

Fig. 9. Using cycle thickness distributions to make inferences of ancient sea level forcing: an example from the mid-Carboniferous Bird Springs Formation in Arrow Canyon, Nevada. (a) Measured stratigraphy, with biostratigraphic timescale from Bishop et al. (2010) and meter 0 defined as the base of the Bird Springs Fm. Meter 0 also corresponds to the start of the brass tags affixed every 1.5 meters by the Amoco Oil Company, which developed a biostratigraphy for the Arrow Canyon section. (b) Fischer diagram of perceived cycles (in this case, defined as runs of coarsening-upward facies). (c) The Ross and Ross (1987) Late Paleozoic eustasy curve (as well as the Veevers and Powell (1987) inferred relative ice volume curve), correlated to our stratigraphic section using the Morrowan-Atokan and Atokan-Desmoinesian stage boundaries (Bishop et al., 2010). (d) The R^2-difference (exponential - lognormal) of cycle thickness distributions computed for a moving window through the stratigraphy. A window size of 40 cycles is chosen in (d), but the curve is relatively insensitive to window size. (e) A few examples of the cycle thickness distributions that make up the curve in (d). Note that the distributions become more exponential (relative to lognormal) from meter 150 to 420. (f-g) Examples of intervals in the Bird Springs Fm that (visually and distributionally) appear more and less cyclic. (h-i) A note of caution: successful application of this method requires that every layer—including the thinnest ones—be logged in the stratigraphic section. Grouping layers of like facies skews thickness distributions towards being more lognormal (i).

4. **Do parasequences record periodic behavior?** Drummond and Wilkinson (1996) articulate a compelling argument against meter-scale parasequences recording orbitally-driven sea level fluctuations—if the thickness distribution of parasequences is non-modal, how could such 'cycles' represent a periodic forcing? In our tile stacking model, we can constrain exactly the thickness of carbonate sediments deposited during each sea level oscillation. The thickness distribution of these cycles is modal and symmetrically-distributed around the expected thickness (period × subsidence rate) (Fig. 6d). However, in the geologic record, it can be difficult to distinguish such 'true' cycles, especially because subaerial exposure surfaces are an inconsistent and unreliable indicator of cycle boundaries (Fig. 7). Instead, cycles defined by classic rules—for example, either (1) assigning a depth rank to each lithofacies (in this case, using our knowledge of the water depth distributions of each facies in Fig. 1: mudstone > wackestone > shelly grainstone > oolitic grainstone > packstone) (Fig. 10a), or (2) assuming that shallowing is characterized by coarsening-upward facies sequences (i.e., mudstone > wackestone > packstone > oolitic grainstone > shelly grainstone)—produce strongly asymmetric distributions. The thickness distributions of such perceived cycles match the observations of Drummond and Wilkinson (1996). In other words, our inability to identify true allocy-

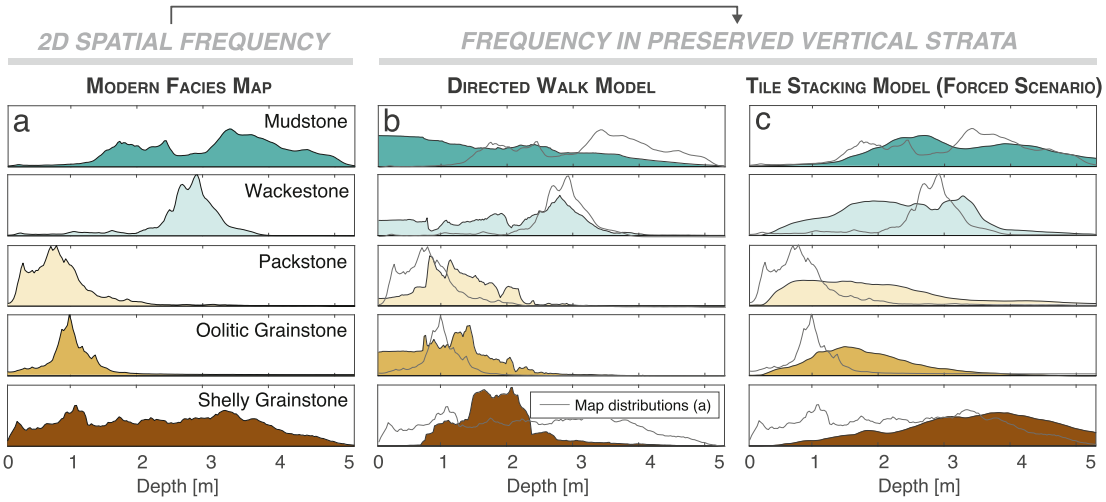

Fig. 10. Water depth distributions of each sedimentary facies in (a) the Andros map (Fig. 1) and (b-c) the simulated stratigraphic columns generated through the directed walk model (Fig. 3) and the tile stacking model (Fig. 4). The differences between (a-c) highlight the fact that the facies and water depth variations on modern carbonate platforms are not necessarily what gets preserved in the rock record. In (b-c), for simplicity, the distributions from just the landward sequences in the case of the directed vs. random walk model and the forced sequences in the tile stacking model are shown. (b) Since the directed walk model prescribes complete filling of the available accommodation space, without a subsequent 'cycle' to erode the top of the sequence, the water depth distributions are skewed towards shallower depths. (c) In contrast, the tile stacking model encodes a dynamic in which shallower sedimentation is more susceptible to be eroded by subsequent local bathymetric deepenings (Fig. 4), favoring the preservation of deeper occurrences of most facies than observed in map view. However, a common feature of b-c is that the predictive power of individual facies in stratigraphic sequences to encode their depositional water depth is *less than* that observed in map view (a).

cles in the stratigraphic record seems to reconcile the apparent dissonance between periodic forcing mechanisms and strongly asymmetric thickness distributions.

5. **Can we distinguish internal vs. external cycles?** In the tile stacking model, shallowing-upward cycles result from both autocyclic (internal) and allocyclic (external) processes (Fig. 6). However, we find that the thickness distribution of perceived cycles (defined by depth rank or coarsening-upwards criteria) is a robust way to distinguish between forced and unforced scenarios (Fig. 8). Our first test of this hypothesis on shallow carbonates from the LPIA shows promising results (Fig. 9). Future high resolution stratigraphic logs (cm-scale observations documenting every layer) of shallow carbonate successions from different periods in Earth history will help test these predictions.

4. Conclusions

Much of our understanding of Earth history comes from shallow water carbonates, and one of the most useful pieces of paleoenvironmental and paleoclimatic information we can extract from this archive is a record of ancient sea level. Cyclic, meter-scale packages of shallow carbonate facies often have been interpreted as representing sea level fall. These shallowing-upwards parasequences form the building block of paleoclimatic interpretations and astrochronological analyses. However, observations from the Bahamas, a modern analog to the shallow carbonate platforms that dominate the geologic record, indicate that true water depth change often does not produce the kinds of canonical parasequences sought out by geologists. We present two findings that suggest it still may be possible to extract ancient relative sea level histories from carbonate strata. First, we show that, by leveraging the information encoded in facies *transitions* in a stratigraphic column, we can determine probabilistically whether a sequence represents relative sea level fall. Second, we acknowledge that local shallowing could arise from either internal platformal mechanisms or external sea level forcing, and try to distinguish between the two. Using a new data-driven tile stacking model that tries to capture how modern facies mosaics evolve to preserve strata, we simulate sedimentary sequences that form during periods of constant and oscillatory sea level. We suggest that the sea level regime imparts a characteristic statistical signature on the thickness distributions of perceived cycles in the resulting sedimentary sequence, providing a new tool for geologists to constrain ancient climate and sea level histories from shallow carbonates.

Declaration of competing interest

The authors declare that they have no known competing financial interests or personal relationships that could have appeared to influence the work reported in this paper.

Acknowledgements

Thank you to Jeff Birch at Small Hope Bay Lodge and the Bahamas Environment, Science & Technology Commission for making work possible on Andros Island. Also thank you to Alex Cartwright, Rudolph 'Timer' Coakley, Niki Hinsey, Tano Humes, Anastasia Mackey, Alvin Marshall, Sonny 'Abba' Martin, Bhruna Neymor, Garnet Thompson, Linda Whyms, and local customs and immigration. Chris Allen at Air Flight Charters and Dawn Reading at Princeton provided logistical support. Thank you to Sujith Ravi for generous access to his laser diffraction particle size analyzer. Thank you to Liam O'Connor and Tano Humes for assistance in the field, to James Bishop for help planning our work in Arrow Canyon, and to Frederik Simons and Akshay Mehra for helpful feedback and advice. Finally, thank you to Bruce Wilkinson and Peter Burgess for detailed reviews. This material is based upon work supported by NSF Division of Earth Sciences Grant 1410317 and by the Princeton Environmental Institute through the Smith-Newton Scholars Program. This work also was supported by the GSA Northeastern Section Stephen G. Pollock Undergraduate Student Research Grant, The Evolving Earth Foundation, the High Meadows Foundation, and the Sigma Xi Research Society. Planet provided the RapidEye satellite imagery through the Planet Research Ambassadors Program (Planet Team, 2017). The Bahamas grain size measurements and the facies and bathymetry maps (Fig. 1) are provided on the data repository Princeton DataSpace (https://doi.org/10.34770/27zb-m284).

Appendix A. Supplementary material

Supplementary material related to this article can be found online at https://doi.org/10.1016/j.epsl.2021.116790.

References

Bishop, J.W., Montañez, I.P., Osleger, D.A., 2010. Dynamic Carboniferous climate change, Arrow Canyon, Nevada. Geosphere 6, 1–34.

Bosence, D.W.J., Wood, J.L., Rose, E.P.F., Qing, H., 2000. Low- and high-frequency sea-level changes control peritidal carbonate cycles, facies and dolomitization in the Rock of Gibraltar (Early Jurassic, Iberian Peninsula). J. Geol. Soc. 157, 61–74.

Burgess, P.M., 2001. Modeling carbonate sequence development without relative sea-level oscillations. Geology, 1127–1130.

Burgess, P.M., 2008. The nature of shallow-water carbonate lithofacies thickness distributions. Geology 36, 235–238.

Burgess, P.M., 2016. Identifying ideal stratigraphic cycles using a quantitative optimization method. Geology 44, 443–446.

Burgess, P.M., Pollitt, D.A., 2012. The origins of shallow-water carbonate lithofacies thickness distributions: one-dimensional forward modelling of relative sea-level and production rate control. Sedimentology 59, 57–80.

Burgess, P.M., Wright, V.P., 2003. Numerical forward modeling of carbonate platform dynamics: an evaluation of complexity and completeness in carbonate strata. J. Sediment. Res. 73, 637–652.

Burgess, P.M., Wright, V.P., Emery, D., 2001. Numerical forward modelling of peritidal carbonate parasequence development: implications for outcrop interpretation. Basin Res. 13, 1–16.

Drummond, C.N., Dugan, P.J., 1999. Self-organizing models of shallow-water carbonate accumulation. J. Sediment. Res. 69, 939–946.

Drummond, C.N., Wilkinson, B.H., 1993a. Aperiodic accumulation of cyclic peritidal carbonate. Geology 21, 1023–1026.

Drummond, C.N., Wilkinson, B.H., 1993b. Carbonate cycle stacking patterns and hierarchies of orbitally forced eustatic sealevel change. J. Sediment. Res. 63, 369–377.

Drummond, C.N., Wilkinson, B.H., 1996. Stratal thickness frequencies and the prevalence of orderedness in stratigraphic sequences. J. Geol. 104, 1–18.

Dunham, R.J., 1962. Classification of carbonate rocks according to depositional texture. In: AAPG: Classification of Carbonate Rocks – A Symposium, pp. 108–121.

Dyer, B., Maloof, A., Purkis, S., Harris, P., 2019. Quantifying the relationship between water depth and carbonate facies. Sediment. Geol. 373.

Fischer, A.G., 1964. The Lofer cyclothems of the Alpine Triassic. Bull.- Kans. Geol. Surv. 169, 107–149.

Ganti, V., Straub, K.M., Foufoula-Georgiou, E., Paola, C., 2011. Space-time dynamics of depositional systems: experimental evidence and theoretical modeling of heavy-tailed statistics. J. Geophys. Res., Earth Surf. 116.

Geyman, E.C., Maloof, A.C., 2019. A simple method for extracting water depth from multispectral satellite imagery in regions of variable bottom type. Earth Space Sci. 6, 527–537.

Ginsburg, R.N., 1971. Landward movement of carbonate mud: new model for regressive cycles in carbonates (abstract). Am. Assoc. Pet. Geol. 55, 340.

Goldhammer, R.K., Dunn, P.A., Hardie, L.A., 1990. Depositional cycles, composite sea-level changes, cycle stacking patterns, and the hierarchy of stratigraphic forcing: examples from Alpine Triassic platform carbonates. Geol. Soc. Am. Bull. 102, 535.

Grotzinger, J.P., 1986. Cyclicity and paleoenvironmental dynamics, Rocknest platform, northwest Canada. Geol. Soc. Am. Bull. 97, 1208–1231.

Harris, P.M.M., Purkis, S.J., Ellis, J., Swart, P.K., Reijmer, J.J.G., 2015. Mapping bathymetry and depositional facies on Great Bahama Bank. Sedimentology 62, 566–589. https://doi.org/10.1111/sed.12159.

Klovan, J.E., 1966. The use of factor analysis in determining depositional environments from grain-size distributions. J. Sediment. Res. 36, 115.

Koerschner, W.F., Read, J.F., 1989. Field and modelling studies of Cambrian carbonate cycles, Virginia, Appalachians. J. Sediment. Res. 59, 654–687.

Lehrmann, D.J., Goldhammer, R.K., 1999. Secular variation in parasequence and facies stacking patterns of platform carbonates: a guide to application of stacking-patterns analysis in strata of diverse ages and settings. In: Advances in Carbonate Sequence Stratigraphy Application to Reservoirs Outcrops and Model. SEPM, pp. 187–225.

Lyzenga, D.R., 1978. Passive remote sensing techniques for mapping water depth and bottom features. Appl. Opt. 17, 379–383.

Manifold, L., Hollis, C., Burgess, P., 2020. The anatomy of a Mississippian (Viséan) carbonate platform interior, UK: depositional cycles, glacioeustasy and facies mosaics. Sediment. Geol.

Medina-Elizalde, M., 2013. A global compilation of coral sea-level benchmarks: implications and new challenges. Earth Planet. Sci. Lett. 362, 310–318.

Mehra, A., Maloof, A., 2018. Multiscale approach reveals that *Cloudina* aggregates are detritus and not in situ reef constructions. Proc. Natl. Acad. Sci. USA 115, E2519–E2527.

Montañez, I.P., Poulsen, C.J., 2013. The late Paleozoic Ice Age: an evolving paradigm. Annu. Rev. Earth Planet. Sci. 41, 629–656.

Osleger, D., Read, J.F., 1991. Relation of eustasy to stacking patterns of meter-scale carbonate cycles, Late Cambrian, U.S.A. J. Sediment. Petrol. 61, 1225–1252.

Peters, S.E., Husson, J.M., 2017. Sediment cycling on continental and oceanic crust. Geology 45, 323–326.

Pollitt, D., Burgess, P., Wright, V., 2015. Investigating the occurrence of hierarchies of cyclicity in platform carbonates. Geol. Soc. (Lond.) Spec. Publ. 404, 123–150.

Purkis, S.J., Harris, P.M., Ellis, J., 2012. Patterns of sedimentation in the contemporary Red Sea as an analog for ancient carbonates in rift settings. J. Sediment. Res. 82, 859–870.

Purkis, S.J., Rowlands, G.P., Kerr, J.M., 2014. Unravelling the influence of water depth and wave energy on the facies diversity of shelf carbonates. Sedimentology, 1–25.

Rabiner, L., Juang, B., 1986. An introduction to Hidden Markov models. IEEE ASSP Mag. 4016.

Rankey, E., 2004. On the interpretation of shallow shelf carbonate facies and habitats: how much does water depth matter? J. Sediment. Res. 74.

Read, J.F., Grotzinger, J.P., Bova, J.A., Koerschner, W.F., 1986. Models for generation of carbonate cycles. Geology 14, 107–110.

Ross, C.A., Ross, J.R., 1987. Late Paleozoic sea levels and depositional sequences. Spec. Pub. – Cushman Found. Foraminifer. Res. 137.

Sadler, P.M., 1981. Sediment accumulation rates and the completeness of stratigraphic sections. J. Geol. 89, 569–584.

Sadler, P.M., Strauss, D.J., 1990. Estimation of the completeness of stratigraphical sections using empirical data and theoretical models. Q. J. Geol. Soc. Lond. 147, 471–485.

Schlager, W., 1981. The paradox of drowned reefs and carbonate platforms. Geol. Soc. Am. Bull. 92, 197–211.

Schumer, R., Jerolmack, D., McElroy, B., 2011. The stratigraphic filter and bias in measurement of geologic rates. Geophys. Res. Lett. 38.

Strasser, A., 1991. Chapter: Lagoonal-peritidal sequences in carbonate environments: autocyclic and allocyclic processes. In: Cycles and Events in Stratigraphy. Springer Verlag, Berlin, pp. 709–721.

Straub, K.M., Duller, R.A., Foreman, B.Z., Hajek, E.A., 2020. Buffered, incomplete, and shredded: the challenges of reading an imperfect stratigraphic record. J. Geophys. Res., Earth Surf. 125.

Tipper, J.C., 1997. Modeling carbonate platform sedimentation, lag comes naturally. Geology 25, 495.

Veevers, J., Powell, C., 1987. Late Paleozoic glacial episodes in Gondwanaland reflected in transgressive-regressive depositional sequences in Euramerica. Geol. Soc. Am. Bull. 98, 475–487.

Walther, J., 1894. Einleitung in die Geologie als historische Wissenschaft. Verlag von Gustav Fisher, Jena, Germany.

Wilkinson, B.H., Drummond, C.N., 2004. Facies mosaics across the Persian Gulf and around Antigua—stochastic and deterministic products of shallow-water sediment accumulation. J. Sediment. Res. 74, 513–526.

Wilkinson, B.H., Drummond, C.N., Diedrich, N.W., Rothman, E.D., 1999. Poisson processes of carbonate accumulation on Paleozoic and Holocene platforms. J. Sediment. Res. 69, 338–350.

Wilkinson, B.H., Drummond, C.N., Rothman, E.D., Diedrich, N.W., 1997. Stratal order in peritidal carbonate sequences. J. Sediment. Res. 67, 1068–1082.